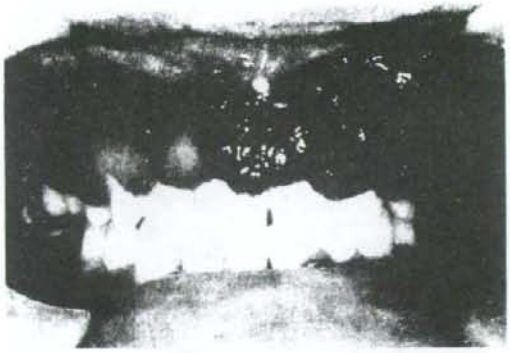

Figure 1. Buccal cavity. The entire maxillary buccal gingival area is swollen, and dark red tumors are observed in a patient with acquired immunodeficiency syndrome (AIDS) and Kaposi's sarcoma (KS).

Figure 2. The right eye. Two dark red, flatly elevated lesions are recognized in the lower lid conjunctiva, and pedunculate lesions are observed in the entire lower conjunctival fornix and medial canthus. Partial hemorrhage is visible.

fragment and visualized by ethidium bromide staining under ultraviolet transillumination.

Serology

An immunofluorescence assay (IFA) was carried out as described previously.[9,10] To detect anti-HHV-8 serum antibodies, we first propagated TY-1 cells by adding 20 ng/ml tetradecanoyl phorbol ester (TPA) to the culture medium for 48 h. After washing twice in PBS, the TPA-induced TY-1 cells were spotted onto a slide (Erie Scientific, Erie, CO, USA), dried, and then fixed in acetone for 10 min at room temperature. The patient's serum was diluted 1:40 in PBS–2% fetal calf serum and applied to the slide for 45 min at room temperature. Rabbit anti-human IgG conjugated

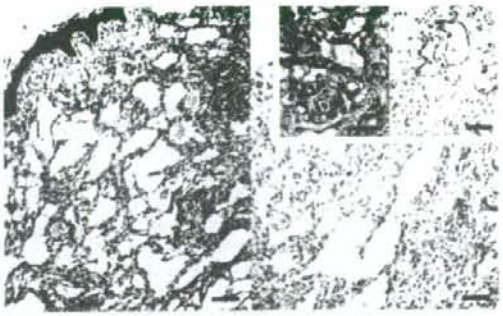

Figure 3. Conjunctival sample. Histopathological findings (H&E staining, *left*) show spindle-shaped cell proliferation and multiple slit-like vessels. A typical swollen endothelial cell is found in the lumen of the slit-like vessels. Among the vessels, spindle-shaped tumor cells are distributed, some showing a fascicular pattern. Bar = 200 μm. Immunohistochemical staining (anti-CD 31, ×40, *right*) shows CD 31-positive cells on the inner surface of the slit-like vessels. Bar = 400 μm. Inset: Bar = 800 μm.

with fluorescein isothiocyanate (Tago Immunologicals, Camarillo, CA, USA) was used as the secondary antibody. Between these steps, the slides were washed three times each in PBS for 5 min. A positive reaction of HHV-8 antibody by IFA was determined by the presence of LANA, other nuclear antigens, and/or cytoplasmic antigens.

Results

Pathology

Tumors were located just below the conjunctival epithelium. Histopathologically, proliferation of spindle-shaped cells and multiple slit-like vessels were observed. Typical swollen endothelial cells lined the lumen of the slit-like vessels. Among these vessels, spindle-shaped tumor cells were distributed, and some of them showed a fascicular pattern (Fig. 3).

Immunohistochemistry

CD 31-positive cells were noted on the inner surface of the slit-like vessels, indicating that the cells forming the slit-like structures were of vascular endothelial cell origin (Fig. 3). Using anti-LANA antibody, dot-shaped staining reactions were observed in the nuclei of the spindle-shaped cells, indicating the presence of the ORF73 protein of HHV-8 in these cells (Fig. 4).

Polymerase Chain Reaction

Agarose gel electrophoresis of the PCR products showed human β-globin DNA (248 bp) in all samples, confirming the

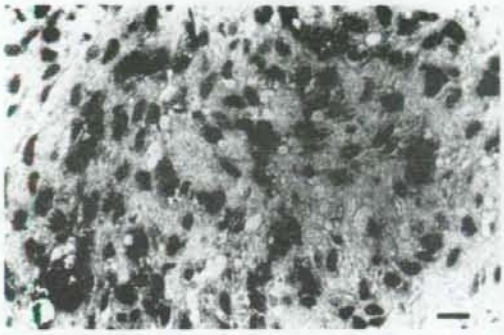

Figure 4. Immunohistochemical staining (anti-latency-associated nuclear antigen, anti-LANA) of the conjunctival sample. Dot-shaped staining reactions are observed in the nuclei of the spindle-shaped cells. Bar = 10μm.

Figure 6. Serum anti-HHV-8 antibodies are detected by an indirect immunofluorescence method using acetone-fixed TY-1 cells, showing mainly LANA in the nuclei. Bar = 10μm.

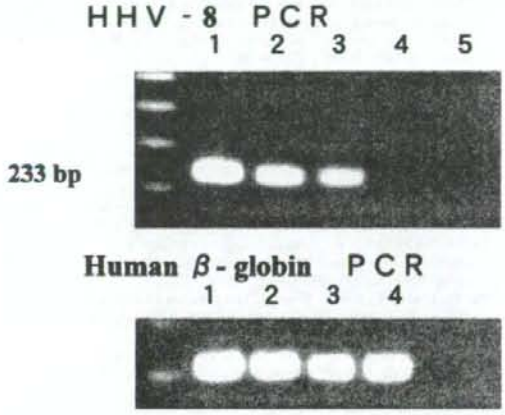

Figure 5. Polymerase chain reaction (*PCR*) analysis using patient's conjunctival KS sample. *Lane 1*, TY-1 cell [human herpesvirus (*HHV*)-8 positive]; *lane 2*, patient's sample 1; *lane 3*, patient's sample 2; *lane 4*, HUVEC (HHV-8 negative); *lane 5*, double sterilized water (negative control). The 233-bp target sequence of HHV-8 is detected in the conjunctival KS tumor and TY-1 cells. *Human β-globin* DNA (248bp) is demonstrated in all samples, confirming the quality of DNA samples.

quality of the DNA samples. The 233-bp target sequence of HHV-8 was detected in the conjunctival KS tumor and in the TY-1 cells (Fig. 5).

Serology

Anti-HHV-8 antibody was detected in the serum, and the antibody titer was estimated to be 1:40 (Fig. 6).

Discussion

Kaposi's sarcoma is the most common neoplasm in patients infected with HIV. Prior to the AIDS epidemic, this tumor was exceedingly rare, but it is now very common, particularly in patients with AIDS. The incidence in homosexual men with AIDS is 20 times that in hemophilic patients,[11] but the pathogenesis of AIDS-related KS is unknown. KS usually occurs when CD4-positive cells decrease to less than 200/μl, but KS has also been reported in a patient with more than 500/μl of CD4.[12] When associated with AIDS, KS is particularly aggressive, affecting mainly the skin and disseminating to visceral organs such as the gastrointestinal tract, lung, and liver. AIDS-associated ocular KS usually occurs in the eyelids or conjunctiva in the late course of the disease. The lesion may be flat or raised at the lower fornix and is bright red and surrounded by tortuous, dilated vessels, resembling subconjunctival hemorrhage. Clinically, ocular KS is classified into three stages.[13] In stages 1 and 2, the tumors are patchy and flat (less than 3mm high) and in stage 3, the tumors are nodular and elevated (more than 3 mm high).

Histologically, stage 1 lesions consist of thin-walled, dilated vascular channels lined with flat endothelial cells, and they are often filled with erythrocytes. Mitotic figures are not usually seen. Features of stage 2 lesions are plump, fusiform cells that form thin-walled, dilated, and empty vascular channels. A number of these cells have hyperchromatic nuclei. Stage 3 lesions are characterized by large aggregates of densely packed spindle cells with slit-like spaces, many of which contain erythrocytes. The lesion of our patient was classified as stage 3, both clinically and histologically.

The treatment of ocular KS depends on the ocular symptoms as well as on the general condition of the patient. If the patient has no ocular symptoms, no local treatment is

required. Surgery is a safer and more effective treatment option, depending on the clinical and histopathological stage of the tumor and its location. Stage 3 KS of the bulbar conjunctiva should be excised surgically, preferably under better visualization of the tumor-associated vessels by fluorescein angiography.

We detected DNA fragments of HHV-8 from the resected conjunctival tissue. In 1994, Chang et al.[4] reported two DNA fragments of 330 bp and 631 bp, which were detected specifically in the KS lesion of AIDS patients by representational difference analysis (RDA). They named them Kaposi's sarcoma-associated herpesvirus-like DNA, owing to DNA homology with herpesvirus saimiri and Epstein-Barr virus. However, the agent has now been determined to be HHV-8, since not only DNA fragments but also whole infective virus have been found in the lesion. Recently, HHV-8 DNA has been identified in KS lesions of various organs such as skin, gastrointestinal tract,[4] lymph node,[14] lung, liver, pericardium, prostate gland,[15] oral mucosa,[16] pancreas, and intestinal tract.[17] However, HHV-8 DNA has not been reported heretofore in an ocular KS lesion.

ORF73 protein antigen is known to appear in the nuclei of cells latently infected by HHV-8. Therefore, the fact that most of the spindle cells, the main component of KS, are positive for ORF73 suggests that HHV-8 exists in a latent state in KS.[6] Our immunohistological examination supported this conclusion, that HHV-8 should be identified as a possible cause of ocular KS.

Serological examination also suggested that HHV-8 was responsible for KS in our patient. The infection route and pathology of HHV-8 are still obscure, but HHV-8 may be sexually transmitted. A previous report showed that anti-HHV-8 serum antibody was positive in 88% of an AIDS-associated KS group, in 30% of an HIV-positive (without KS) group, and in 1%–4% of a normal group.[18] Additionally, the antibody titer of the sexually transmitted HIV group was markedly higher than that of the HIV group with other routes of infection.[19] It has also been reported that the appearance of anti-HHV-8 antibody precedes the onset of KS.[20] Our patient was also a homosexual man without a history of transfusion or surgery, and he was serologically positive for HHV-8. Recently, ORF73 has been observed in conjunctival KS.[21] Our detailed analyses of the present case further provide histological, DNA and serological evidence more directly linking HHV-8 to the pathogenesis of conjunctival KS. Since ocular KS is still rarely encountered in Japan, our comprehensive coverage of ocular and systemic lesions may provide ophthalmologists and general physicians with a more complete clinical profile of KS in AIDS patients. KS is a treatable disease if diagnosed promptly. However, specific treatment for KS has not yet been established. New effective agents that not only promote regression of KS lesions but also prevent recurrence are needed at present.

Acknowledgments. The authors appreciate the helpful suggestions by Dr. M. Usui. We also thank Dr. K. Fukutake for editorial assistance.

References

1. Beral V, Peterman TA, Berkelman RL, Jaffe HW. Kaposi's sarcoma among persons with AIDS: a sexually transmitted infection? Lancet 1990;335:123–128.
2. Havercos HW, Drotman DP. Prevalence of Kaposi's sarcoma among patients with AIDS. N Engl J Med 1985;312:1518.
3. Jabs DA, Quinn TC. Acquired immunodeficiency syndrome. In: Pepose JS, Holland GN, Wilhelmus KR, editors. Ocular Infection and Immunity. St. Louis: Mosby, 1996; p. 289–310.
4. Chang Y, Cesarman E, Pessin MS, et al. Identification of herpesvirus-like DNA sequences in AIDS-associated Kaposi's sarcoma. Science 1994;266:1865–1869.
5. Parums DV, Cordell JL, Micklem K, et al. JC70: a new monoclonal antibody that detects vascular endothelium associated antigen on routinely processed tissue sections. J Clin Pathol 1990;43:752–757.
6. Katano H, Sato Y, Kurata T, et al. High expression of HHV-8-encoded ORF73 protein in spindle-shaped cells of Kaposi's sarcoma. Am J Pathol 1999;155:47–52.
7. Katano H, Morishita Y, Cui LX, et al. Expression of latent membrane protein 1 in clinically isolated cases and animal models of AIDS-associated non-Hodgkin's lymphomas. Pathol Int 1996;46:568–574.
8. Katano H, Hoshino Y, Morishita Y, et al. Establishing and characterizing a CD30-positive cell line harboring HHV-8 from a primary effusion lymphoma. J Med Virol 1999;58:394–401.
9. Kedes DH, Ganem D, Ameli N, et al. The prevalence of serum antibody to human herpesvirus 8 (Kaposi's sarcoma-associated herpesvirus) among HIV-seropositive and high risk HIV seronegative women. JAMA 1997;277:478–481.
10. Simpson GR, Schulz TF, Whitby D, et al. Prevalence of Kaposi's sarcoma associated herpesvirus infection measured by antibodies to recombinant capsid protein and latent immunofluorescence antigen. Lancet 1996;348:1133–1138.
11. Beral V, Bull D, Darby S, et al. Risk of Kaposi's sarcoma and sexual practices associated with faecal contact in homosexual or bisexual men with AIDS. Lancet 1992;339:632–635.
12. Orfanos CE, Husak R, Wölfer U, et al. Kaposi's sarcoma: a reevaluation. Recent Results Cancer Res 1995;139:275–296.
13. Dugel PU, Gill PS, Frangieh GT, et al. Ocular adnexal Kaposi's sarcoma in acquired immunodeficiency syndrome. Am J Ophthalmol 1990;110:500–503.
14. Su I, Hsu Y, Chang Y, et al. Herpesvirus-like DNA sequence in Kaposi's sarcoma from AIDS and non-AIDS patients in Taiwan. Lancet 1995;345:722–723.
15. Corbellino M, Poirel L, Bestetti G, et al. Restricted tissue distribution of extralesional Kaposi's sarcoma-associated herpesvirus-like DNA sequences in AIDS patients with Kaposi's sarcoma. AIDS Res Hum Retroviruses 1996;12:651–657.
16. Webster-Cyriaque J, Edwards RH, Quinlivan EB, et al. Epstein-Barr virus and human herpesvirus 8 prevalence in human immunodeficiency virus associated oral mucosal lesions. J Infect Dis 1997;175:1324–1332.
17. Cathomas G, Stalder A, McGandy CE, et al. Distribution of human herpesvirus 8 DNA in tumorous and nontumorous tissue of patients with acquired immunodeficiency syndrome with and without Kaposi's sarcoma. Mod Pathol 1998;11:415–420.
18. Gao SJ, Kingsley L, Li M, et al. KSHV antibodies among Americans, Italians and Ugandans with and without Kaposi's sarcoma. Nat Med 1996;2:925–928.
19. Kedes DH, Operskalski E, Busch M, et al. The seroepidemiology of human herpesvirus 8 (Kaposi's sarcoma-associated herpesvirus): distribution of infection in KS risk groups and evidence for sexual transmission. Nat Med 1996;2:918–924.
20. Gao SJ, Kingsley L, Hoover DR, et al. Seroconversion to antibodies against Kaposi's sarcoma-associated herpesvirus-related latent nuclear antigens before the development of Kaposi's sarcoma. N Engl J Med 1996;335:233–241.
21. Hasche H, Eck M, Lieb W. Immunochemical demonstration of human herpesvirus 8 in conjunctival Kaposi's sarcoma [in German]. Ophthalmologe 2003;100:142–144.

Journal of Pathology
J Pathol 2006; **209**: 464–473
Published online 1 June 2006 in Wiley InterScience
(www.interscience.wiley.com) **DOI:** 10.1002/path.2012

Original Paper

Effusion and solid lymphomas have distinctive gene and protein expression profiles in an animal model of primary effusion lymphoma

Y Yanagisawa,[1] Y Sato,[2] Y Asahi-Ozaki,[2] E Ito,[1] R Honma,[1] J Imai,[1] T Kanno,[1] M Kano,[2] H Akiyama,[3] T Sata,[1] F Shinkai-Ouchi,[1] Y Yamakawa,[3] S Watanabe[1] and H Katano[2]*

[1] Department of Clinical Research, Tokyo Medical and Dental University, Tokyo, Japan
[2] Department of Pathology, National Institute of Infectious Diseases, Tokyo, Japan
[3] Department of Biochemistry and Cell Biology, National Institute of Infectious Diseases, Tokyo, Japan

*Correspondence to: Dr H Katano, Department of Pathology, National Institute of Infectious Diseases, 1-23-1 Toyama, Shinjuku, Tokyo 162-8640, Japan.
E-mail: katano@nih.go.jp

Abstract

Lymphoma usually forms solid tumours in patients, and high expression levels of adhesion molecules are observed in these tumours. However, Kaposi's sarcoma-associated herpesvirus (KSHV)-related primary effusion lymphoma (PEL) does not form solid tumours and adhesion molecule expression is suppressed in the cells. Inoculation of a KSHV-associated PEL cell line into the peritoneal cavity of severe combined immunodeficiency mice resulted in the formation of effusion and solid lymphomas in the peritoneal cavity. Proteomics using two-dimensional difference gel electrophoresis and DNA microarray analyses identified 14 proteins and 105 genes, respectively, whose expression differed significantly between effusion and solid lymphomas. Five genes were identified as having similar expression profiles to that of lymphocyte function-associated antigen 1, an important adhesion molecule in leukocytes. Among these, coronin 1A, an actin-binding protein, was identified as a molecule showing high expression in solid lymphoma by both DNA microarray and proteomics analyses. Western and northern blotting showed that coronin 1A was predominantly expressed in solid lymphomas. Moreover, KSHV-encoded lytic proteins, including viral interleukin-6, were highly expressed in effusion lymphoma compared with solid lymphoma. These data demonstrate that effusion and solid lymphomas possess distinctive gene and protein expression profiles in our mouse model, and suggest that differences in gene and protein expression between effusion and solid lymphomas may be associated with the formation of effusion lymphoma or invasive features of solid lymphoma. Furthermore, the results obtained using this combination of proteomics and DNA microarray analyses indicate that protein synthesis partly reflects, but does not correlate strictly with, mRNA production.

Received: 26 December 2005
Revised: 7 March 2006
Accepted: 17 April 2006

Keywords: primary effusion lymphoma; animal model; proteomics; DNA microarray; Kaposi's sarcoma-associated herpesvirus

Introduction

Primary effusion lymphoma (PEL), also known as body cavity-based lymphoma (BCBL), is a rare complication in patients with acquired immunodeficiency syndrome (AIDS) [1–4], and has a unique character compared with other types of lymphoma. While all other types of lymphoma form solid tumours in lymph nodes or extranodal sites, PEL cells proliferate in the peritoneal, abdominal or pericardial cavity of patients as lymphomatous effusions [2]. Curiously, PEL rarely progresses to leukaemia, and PEL cells prefer to grow as effusions in these body cavities [2]. PEL is known to be associated with Kaposi's sarcoma-associated herpesvirus (KSHV, human herpesvirus 8) infection [1,2,4]. KSHV-encoded latency-associated nuclear antigen (LANA, ORF73) is detected in the nucleus of almost all PEL cells, suggesting that KSHV infects PEL cells in the latent phase [5–7]. KSHV infection is also associated with a type of solid lymphoma (KSHV-associated solid lymphoma) [5,8], which occurs in the skin, lungs and gastrointestinal tract of AIDS patients with homosexual behaviour and sometimes complicates other KSHV-associated diseases, such as Kaposi's sarcoma, PEL, and multicentric Castleman's disease [5]. Since KSHV-associated solid lymphoma possesses similar expression profiles of cellular and viral proteins to PEL, KSHV-associated solid lymphoma is thought to be an extra-cavity variant of PEL [8,9]. Although the molecular biological differences between PEL and KSHV-associated solid lymphoma remain unknown, PEL shows some unique characteristics in its clinical course compared with KSHV-associated solid lymphoma. For example, PEL

cells do not usually demonstrate marked invasion of the peritoneal or pleural membrane, whereas KSHV-associated solid lymphoma often exhibits massive invasion of other organs [2,8–10]. Although the role of KSHV in the formation of solid or effusion lymphoma is currently unknown, the expression of adhesion molecules, such as lymphocyte function-associated antigen type 1 (LFA-1), is likely to be essential for solid lymphoma formation [11–13].

In general, adhesion molecules are expressed on the surface of almost all types of lymphoma cell [13,14]. LFA-1 is the most important molecule involved in lymphocyte adhesion. Almost all leukocytes express LFA-1 on their cell surface, and its mechanism of activation has been elucidated in T cells. Briefly, LFA-1 is activated by stimulation of Rap 1-RAPL from T cell receptors [15], and also by chemokines through the small GTPase RhoA and atypical zeta protein kinase C [16]. When LFA-1 becomes activated, it moves on the cell surface (polarization and redistribution) [17]. Expression of LFA-1 has been reported in various other cell types, including lymphoma cells [18,19]. Epstein–Barr virus-encoded latent membrane protein 1 up-regulates LFA-1 in infected cells [19–21]. Some adult T cell leukaemia cells show low expression of the LFA-1 β-chain (CD18) [22,23]. Thus, some viral infections regulate the expression of LFA-1, although the mechanism of this regulation remains unknown. Since LFA-1 expression is down-regulated in PEL cell lines [11,24–26], this suppression of LFA-1 expression should contribute to the unique features of PEL.

Here, we established an animal model that produced both effusion and solid lymphomas from a KSHV-associated PEL cell line [10]. Using proteomics and DNA microarray analyses, we investigated the differences in the gene and protein expression profiles between effusion and solid types of KSHV-associated lymphoma in this animal model.

Materials and methods

Inoculation of the PEL cell line TY-1 into severe combined immunodeficiency (SCID) mice

TY-1 [27], a KSHV-positive PEL cell line, was injected into the abdominal cavity of 8–10-week-old CB-17 SCID mice [10]. A total of 1×10^7 cells was inoculated into each mouse. All animal procedures were approved by the Animal Care and Use Committee of the National Institute of Infectious Diseases (NIID, Approval No 205091), and were conducted according to 'the Guidelines for Animal Experiments Performed at the NIID'.

Two-dimensional difference gel electrophoresis (2D-DIGE)

2D-DIGE, gel image analysis and matrix-assisted laser desorption ionization/time-of-flight (MALDI-ToF) mass spectrometry were performed as described [28–30]. Details of these procedures are described in the supplementary material (http://www.interscience.wiley.com/jpages/0022-3417/suppmat/path.2012.html).

RNA preparation and DNA microarray

RNA preparation and DNA microarray analysis (MicroDiagnostic, Tokyo, Japan) was performed as previously described [31,32] (supplementary methods, available at http://www.interscience.wiley.com/jpages/0022-3417/suppmat/path.2012.html).

Western blotting

Cell extract preparation and immunoblotting analyses were performed as described [5]. Aliquots of 50 µg protein/lane were separated by sodium dodecyl sulphate–polyacrylamide gel electrophoresis (SDS–PAGE), and probed with anti-LFA-1 (BD Biosciences Pharmingen, San Diego, CA, USA), anti-coronin (Upstate Biotechnology, Lake Placid, NY, USA), anti-vIL-6 [5], anti-ORF59 [5] or anti-Lyn (Santa Cruz Biotechnology, Santa Cruz, CA, USA) antibodies.

Real-time PCR

The amounts of KSHV mRNA and DNA were determined by quantitative real-time (TaqMan) polymerase chain reaction (PCR) using an ABI Prism 7900 HT sequence detection system (Applied Biosystems, Foster City, CA, USA) as described [33–35]. The probe sequences, primer sequences, and real-time PCR details are described in the supplementary methods available at http://www.interscience.wiley.com/jpages/0022-3417/suppmat/path.2012.html.

Results

Establishment of an animal model for effusion and solid lymphomas

We previously reported that inoculation of a PEL cell line, TY-1, resulted in solid lymphoma formation in the peritoneal cavity of SCID mice (Figure 1A) [10,27]. Some of these SCID mice also showed effusion lymphoma formation in their peritoneal cavity. We separately collected both effusion and solid lymphoma components, and inoculated effusion lymphoma cells into the peritoneal cavity of some SCID mice and solid lymphoma cells into subcutaneous sites of other SCID mice. After 3–4 weeks, the effusion lymphoma-inoculated mice showed ascites including effusion lymphoma, whereas the solid lymphoma-inoculated mice developed subcutaneous tumours composed of TY-1 cells. These lymphomas were transplanted six times until the 7th passage (Figure 1B). During the passages, inoculation of effusion lymphoma cells into the peritoneal cavity formed not only effusion lymphoma but also solid lymphoma in the

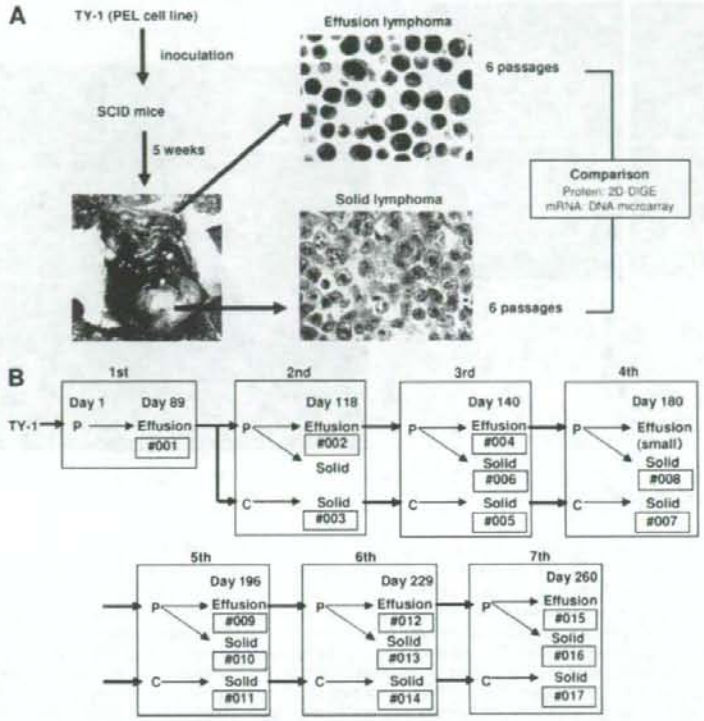

Figure 1. Animal model of effusion and solid lymphomas. (A) Experimental procedure. TY-1, a PEL cell line, was inoculated into the peritoneal cavity of SCID mice. After 5 weeks, effusion and solid lymphomas were obtained from the cavity. These lymphomas were inoculated into other SCID mice. Finally, the protein and gene expression profiles of the two types of lymphoma were compared by 2D-DIGE (proteomics) and DNA microarray analyses. (B) Passages and sample numbers in the present study. Inoculation of effusion lymphoma into other SCID mice resulted in the formation of not only effusion lymphoma but also solid lymphoma in the peritoneal cavity. Samples were taken from both and the sample numbers are shown as #001–017. P = peritoneal cavity; C = subcutaneous

peritoneal cavity in some mice (sample Nos 6, 8, 10, 13, and 16 in Figure 1B). The solid lymphoma-inoculated mice did not develop effusion lymphoma in any of their cavities. Immunohistochemistry revealed that both the effusion and solid lymphomas in SCID mice expressed hCD45, hCD30, and KSHV-LANA [10,36], indicating that the origin of the lymphoma cells was TY-1 [27].

Proteomics of effusion and solid lymphomas

To investigate the differences in the protein expression profiles between effusion and solid lymphomas, effusion and solid lymphoma cells of the 2nd, 3rd, 5th, and 6th passages (sample Nos 2, 4, 9, and 12 [effusion] and 3, 5, 11, and 14 [solid] in Figure 1B, respectively) were collected and lysed in lysis buffer. The lysates were labelled with CyDyes and applied to 2D-DIGE [29]. DeCyder, an image analysis software program, identified 23 spots as proteins showing differences in expression between effusion and solid lymphomas. Among these, 14 and nine spots were identified as proteins showing higher expression in solid and effusion tumours, respectively. All 23 spots were excised from the gels after staining with Coomassie brilliant blue. The proteins in these spots were digested with trypsin, and identified by MALDI-ToF mass spectrometry (Figure 2). Finally, eight and seven proteins were identified as showing higher expression in effusion and solid lymphomas, respectively (supplementary Table 1 at http://www.interscience.wiley.com/jpages/0022-3417/suppmat/path.2012.html). One of these was a mouse protein, but the others were all of human origin. The proteins in the other eight spots could not be identified by mass spectrometry owing to their low levels.

Differential analysis using a DNA microarray

mRNA was extracted from effusion and solid lymphoma samples (sample Nos 1–14), and differences in the mRNA expression profiles were investigated using a DNA microarray containing 28 654 human genes. The DNA microarray identified 105 genes whose

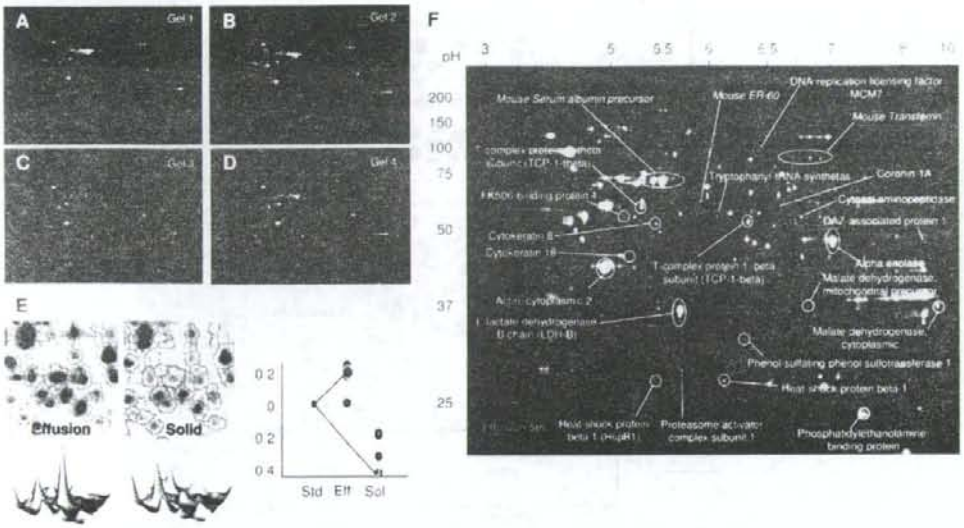

Figure 2. Proteomics of effusion and solid lymphomas. (A–D) Images of 2D-DIGE for the 2nd, 3rd, 5th, and 6th passages of the lymphomas. Proteins from effusion lymphoma were labelled with Cy2 (green) in gel 1 (2nd passage) and gel 3 (5th passage), but Cy3 (red) in gel 2 (3rd passage) and gel 4 (6th passage). Proteins from solid lymphoma were labelled with different colours from effusion lymphoma. (E) Examples of computerized analysis using the DeCyder™ software. The software automatically recognizes all the protein spots on the 2D-DIGE images (upper panels). It then calculates the peak of each protein and draws three dimensional images (lower panels). The peaks were automatically compared among the four gels. Finally, a graph of the protein expression levels in effusion and solid lymphomas (right panel) is created. See text and 'Supplementary methods' (http://www.interscience.wiley.com/jpages/0022-3417/suppmat/path.2012.html) for details. (F) Images of 2D-DIGE and results of MALDI-ToF mass spectrometry. Green and red circles indicate protein spots showing significantly higher expression in effusion and solid lymphomas, respectively. Yellow circles indicate protein spots showing similar expression in both effusion and solid lymphomas.

expression differed by more than two-fold between solid and effusion lymphomas with p-values of <0.005 by t-tests (Figure 3A and supplementary data at http://www.interscience.wiley.com/jpages/0022-3417/suppmat/path.2012.html). Among these, 49 and 56 genes were identified as showing higher expression in effusion and solid lymphomas, respectively (supplementary Table 2 at http://www.interscience.wiley.com/jpages/0022-3417/suppmat/path.2012.html). The group showing predominant expression in effusion lymphoma contained transactivator/cell cycle-associated genes (MAPKAPK2, C/EBPD, G protein-coupled receptor, RRAS, etc), enzymes (ATPase, arginase, lipase, etc), and a cell surface antigen (CD68) (Table 1). The group showing predominant expression in solid lymphoma contained structural proteins (collagens, proteoglycans), adhesion molecules (integrins) and cell cycle-associated genes (MAPKs, IRF1, etc.). In particular, several kinds of collagen were identified as genes predominantly expressed in solid lymphoma.

Comparison of the proteomics and DNA microarray results

Some molecules were identified by both the proteomics and DNA microarray analyses. However, there were also discrepancies between the two sets of results. Therefore, we compared the mRNA levels identified by the DNA microarray and the protein levels identified by the proteomics analysis (supplementary Table 1 at http://www.interscience.wiley.com/jpages/0022-3417/suppmat/path.2012.html). The human proteins with higher expression in solid lymphoma identified by the proteomics analysis (Nos 1–4, 6, and 7 in supplementary Table 1) showed similar expression patterns in the DNA microarray. In contrast, only six of eight proteins with higher expression in effusion lymphoma identified by the proteomics analysis (Nos 8–15 in supplementary Table 1) showed similar trends in the DNA microarray (Nos 9–11 and 13–15). Thus, although the two assays produced similar trends between the two lymphomas, suggesting that mRNA expression correlated with expression of the corresponding proteins, some of the differences in mRNA production detected between the two groups were not significant at the protein level, suggesting that protein expression did not correlate fully with the production of mRNA for these proteins.

Molecules with similar expression profiles to LFA-1

LFA-1 is a major adhesion molecule in lymphocytes [13,14], and its down-regulation plays an

Table 1. Summary of gene and protein expression between effusion and solid lymphomas

	Higher expression in effusion lymphoma	Higher expression in solid lymphoma
Structural or matrix protein	Mucins, JWA	Collagens, CSPG2, LOXL1, **SPARC**, BGN, Coronin, AEBP1, H1F0
Transactivator Cell cycle-associated	MAPKAPK2, C/EBPD, RAS	MAPKs, IGFBP7, IRF1, MCM7
Cell surface membrane protein	CD68, cathepsin B, EMP1, DAF, CAV1, GPR25,	ITM2C, Integrins (ITGAM, **LFA-1**), FUT7
Enzymes	DHRS3, ATPase, arginase, lipase, P-PST, malate dehydrogenase, FK506-BP4	ADA, ACY-3, PTP4A3, ATP2A1, PLCG2, TrpRS, LAP
Others	HSP27, keratins, PEBP, etc	**RBP1, SQLE**, C4B, DAZ-associated protein, PA28a, etc

Genes/proteins identified as showing higher expression in effusion or solid lymphomas are listed. Genes/proteins with unknown function are not listed. Proteins identified by proteomics are underlined. Italics indicate genes/proteins identified by both DNA microarray and proteomics. Bold indicates genes with similar expression profiles to LFA-1.

important role in the pathogenesis of PEL [11]. Immunohistochemistry detected no LFA-1 expression in effusion lymphoma and relatively high expression in solid lymphoma (Figures 4A and B). We attempted to identify genes with similar expression patterns to LFA-1. Cluster analysis of the DNA microarray results based on expression of the 105 identified genes revealed that at least five of the genes belonged to the same cluster as LFA-1 (Figure 3B), suggesting that they had similar expression profiles to LFA-1. Among these five genes, coronin 1A was also identified by proteomics as a protein showing high expression in solid lymphoma. Thus, we investigated the expression of LFA-1 and coronin 1A in effusion and solid lymphomas (Figure 4). Western blotting demonstrated that both LFA-1 and coronin 1A expression was increased during passages in solid lymphoma (Figure 4C). Effusion lymphoma did not express LFA-1, but showed weak expression of coronin 1A (Figure 4C). Northern blot analysis demonstrated that coronin 1A was expressed in solid lymphoma, but not in effusion lymphoma (Figure 4D). These data suggest that coronin 1A has a similar expression profile to LFA-1 in this animal model of effusion and solid lymphomas.

Viral gene and protein expression

Next, we investigated the expression of KSHV-encoded genes and proteins. Real-time PCR analysis demonstrated that the viral interleukin (vIL)-6 transcript showed approximately seven-fold higher expression in effusion lymphoma than in solid lymphoma (Figure 4F). The mRNA copy numbers for ORF50 and ORF73 were also higher in effusion lymphoma than in solid lymphoma (Figures 4E and G). The viral load of KSHV was investigated by real-time PCR analysis for ORF26 DNA (Figure 4H). The results demonstrated that the viral genome titres were lower in solid lymphoma than in effusion lymphoma. Western blotting showed that vIL-6 was only expressed in effusion lymphoma, while LFA-1 and coronin 1A were predominantly expressed in solid lymphoma. The expression of ORF59, a lytic protein of KSHV, decreased during the passages, but did not differ significantly between effusion and solid lymphomas (Figure 4C). Northern blotting also revealed a high level of vIL-6 expression in effusion lymphoma (Figure 4D). Although LANA was expressed in both effusion and solid lymphomas throughout all passages by immunohistochemistry (data not shown), these data suggest that KSHV was activated in effusion lymphoma, but not in solid lymphoma.

Discussion

PEL has unique features compared with all other subtypes of lymphoma [2,4], since its growth is usually restricted to one body cavity and it does not develop into leukaemia or metastasis. Although PEL cells show slight invasion of body cavity walls, such as the pleural or peritoneal membrane, marked invasion and solid tumour formation are rarely found. These features of PEL are dependent on the low expression of adhesion molecules [11,24–26]. Low or absent adhesion molecule expression should contribute to the formation of such an effusion phenotype. On the other hand, KSHV-associated solid lymphoma progresses rapidly and invades various organs, such as the gastrointestinal tract, lungs, and skin [8–10]. Thus, these two lymphomas have distinctive clinical courses, although their cells show similar protein expression patterns, suggesting an identical origin [8,9]. In the present study, 105 of 28 654 genes in a DNA microarray were identified as genes showing differences in expression between effusion and solid lymphomas. Proteomics also identified 14 proteins with differences in expression between the two lymphomas. Therefore, although our data showed that the cellular gene expression profiles of these two lymphomas were very similar, distinctive expression profiles of some genes and proteins were identified between effusion and solid lymphomas in our mouse model. Since the KSHV-associated solid lymphoma cells used in our mouse

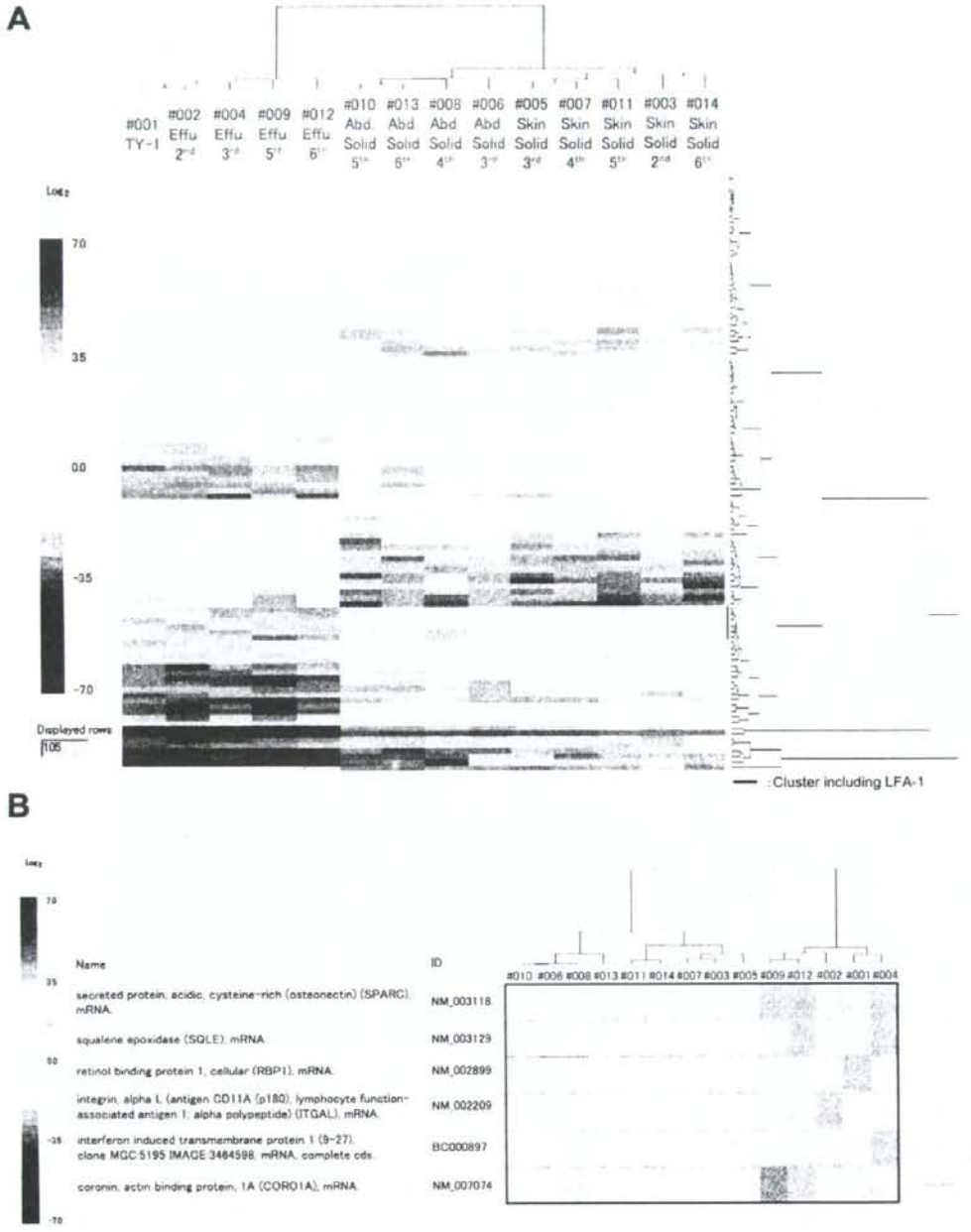

Figure 3. Cluster analysis and gene expression profiles in effusion and solid lymphomas. (A) Cluster analysis. The analysis was based on the expression profile of 105 genes identified as showing differences in expression between effusion and solid lymphomas by DNA microarray analyses. All 105 genes are shown and each row indicates the expression ratios of an individual gene in various samples. Red and blue colours indicate high and low expression, respectively, compared with the human common reference RNA sample. The sample numbers at the top correspond to the numbers in Figure 1B. The blue lines at the top and on the right indicate clusters. A violet line indicates a cluster including LFA-1. The raw data of the DNA microarray are available as supplementary Table 3 at http://www.interscience.wiley.com/jpages/0022-3417/suppmat/path.2012.html. (B) A cluster including LFA-1. Six genes are listed

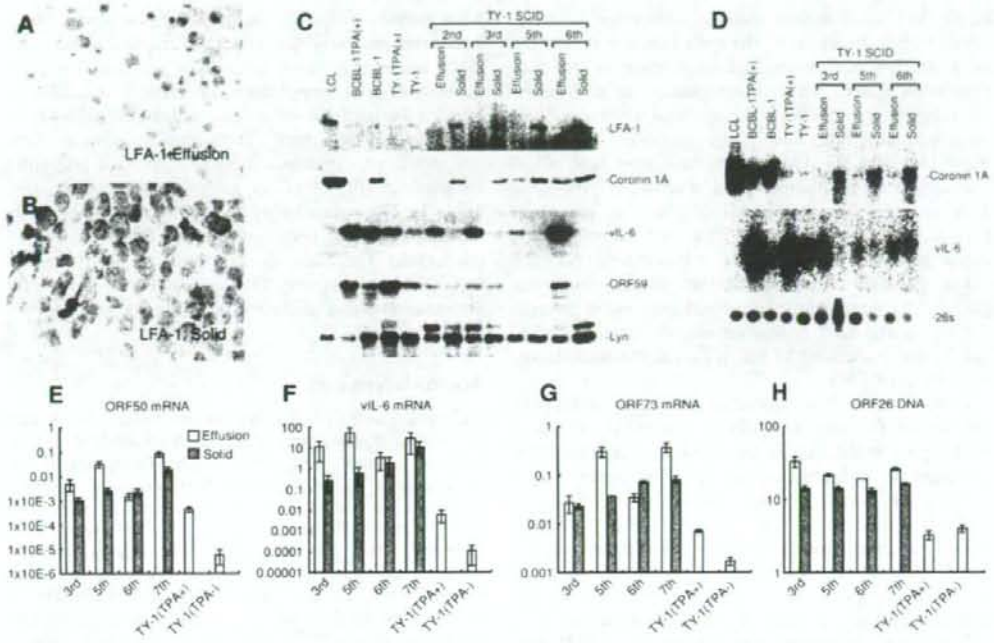

Figure 4. Expression of LFA-1, coronin 1A, and KSHV-encoded genes/proteins in effusion and solid lymphomas. (A, B) Immunohistochemistry of LFA-1. LFA-1 is expressed in solid lymphoma (B), but not in effusion lymphoma (A). (C) Western blotting. LFA-1, coronin 1A, KSHV-encoded vIL-6, and ORF59 were detected. Lyn was examined as an internal control. LCL = lymphoblastoid cell line. (D) Northern blotting. Coronin 1A and KSHV-encoded vIL-6 were detected. 28S ribosomal RNA is shown at the bottom. (E–G) Real-time reverse transcriptase (RT)-PCR for the KSHV-encoded ORF50, vIL-6, and ORF73 genes. The y-axis shows the copy numbers per cell. Effusion and solid lymphomas in the 3rd (sample Nos #004 and #005 in Figure 1B), 5th (#009 and #011), 6th (#012 and #014), and 7th (#015 and #017) passages were examined. The ratios to *GAPDH* mRNA are shown. The error bars indicate the standard deviations. (H) Real-time PCR for virus ORF26 DNA. The ratios to *GAPDH* DNA are shown. The y-axis shows the copy numbers per cell

model show a similar protein expression pattern to KSHV-associated solid lymphoma in humans [10], the results suggest that KSHV-associated solid lymphoma may also be categorized as a different disease entity from PEL in humans. Further studies of human cases are required to clarify the distinctive profiles. In addition, the genes and proteins with different expression profiles between effusion and solid lymphomas may be associated with the formation of effusion lymphoma or invasive features of solid lymphoma. Although some of the genes and proteins are categorized as adhesion molecules, many others have different or unknown functions (Table 1). The list of genes with different expression profiles identified in the present study will be useful for future analyses.

Signal transduction involving LFA-1 activation has been extensively investigated in T cells [15–17,37,38]. Activation of LFA-1 on the cell surface plays roles in various lymphocyte functions, especially adhesion. However, activation is different from expression. PEL cells do not express LFA-1 at all. LFA-1 expression is common among subtypes of lymphoma, but its down-regulation is rare and has only been reported in a few cases of lymphoma. For example, a few cell lines derived from adult T cell leukaemia/lymphoma do not express LFA-1, but do express other adhesion molecules, such as LFA-3 and intercellular adhesion molecule-1 (ICAM-1) [22,23]. Although some adhesion molecules are expressed by PEL cells [39], low expression of LFA-1 seems to be common in PEL cells, and such a restricted expression of LFA-1 may be important for the formation of effusion lymphoma [11,24–26]. Our mouse model of effusion and solid lymphomas was established by inoculating a single cell line originating from a single clone, implying that the origins of the two types of lymphoma were identical. Therefore, what factor could alter gene expression in this model? Endogenous factors, such as autocrine stimulation of cytokines, and exogenous factors, such as viral infection, can be considered. Cytokines and chemokines are known to be associated with the expression of adhesion molecules in cells [38], and to have various effects on adhesion molecules, including their induction and suppression. In our animal model, effusion lymphoma cells grew as peritoneal effusions that should have contained abundant cytokines. For the solid lymphoma inoculated into subcutaneous sites of SCID mice, different kinds of cytokines should

J Pathol 2006; **209**: 464–473 DOI: 10.1002/path

be present between the peritoneal cavity and subcutaneous tissue. In addition, the cells inoculated into the skin attached and stimulated each other in the subcutaneous space, which may induce the expression of adhesion molecules and structural proteins. Viral infection sometimes alters the expression of adhesion molecules [20,21]. Our results indicated that vIL-6 was expressed at a higher level in effusion lymphoma than in solid lymphoma. vIL-6 plays an important role in the pathogenesis of PEL and Kaposi's sarcoma [40–42]. Although the relationships between vIL-6 and adhesion molecules remain unknown, our data clearly demonstrate reciprocal expression patterns for vIL-6 and LFA-1. Further studies are required to clarify the association of vIL-6 expression with down-regulation of LFA-1.

Coronin was first identified as an actin-binding protein in *Dictyostelium discoideum* [43]. It has a WD-repeat motif that is involved in cell migration, cytokinesis, and phagocytosis [44]. Coronin 1A, a mammalian homologue of coronin, is expressed in haematopoietic tissues [43]. It contains five consecutive WD-repeat motifs within its *N*-terminal region and a leucine zipper domain at the *C*-terminus. In mouse T lymphocytes, coronin is involved in the dynamics of the actin cytoskeleton in response to T cell receptor stimulation and cell activation [45]. Our data demonstrated a much higher coronin 1A expression level in solid lymphoma than in effusion lymphoma, and its expression pattern was similar to that of LFA-1. To investigate the expression of coronin 1A in human clinical samples of solid lymphoma, we performed immunohistochemistry on solid lymphoma samples from 12 cases. Coronin 1A was found to be expressed in all samples (data not shown), suggesting that its expression is common in solid lymphoma. Since LFA-1 is also activated by T cell receptor stimulation [37], coronin 1A may be activated by a similar signal transduction mechanism to LFA-1 in solid lymphoma. Interestingly, coronin 1A expression was elevated in BCBL-1 cells, regardless of 12-*O*-tetradecanoylphorbol-13-acetate (TPA) stimulation, but not in TY-1 cells (Figure 4). However, TY-1 cells expressed coronin 1A in the form of a solid lymphoma, suggesting that coronin 1A expression is not strictly associated with TPA stimulation. Furthermore, LFA-1 was not induced in BCBL-1 and TY-1 cells by TPA. Therefore, these data suggest the presence of a specific signal transduction mechanism that induces both LFA-1 and coronin 1A.

Proteomics and DNA microarray analyses are useful tools for comparing gene and protein expression profiles, respectively. However, few studies have used both methods to investigate differences in the gene and protein expression profiles of the same samples [46–48]. The combination of proteomics and DNA microarray analyses of the same samples provided us with new insights into the relationship between mRNA production and protein synthesis. Although coronin 1A was identified by both methods, other molecules were only identified by one method. However, when compared precisely, the results of the proteomics and DNA microarray analyses appeared to correlate with each other well (supplementary Table 1, available at http://www.interscience.wiley.com/jpages/0022-3417/suppmat/path.2012.html). Both methods detected similar trends of expression between effusion and solid lymphomas for 12 of 13 molecules (supplementary Table 1). These data imply that protein synthesis partly reflects, but does not correlate strictly with, mRNA production. Therefore, the combination of proteomics and DNA microarray analyses will provide useful information for elucidating accurate expression profiles of molecules.

Acknowledgements

We thank Mami Matsuda and Tetsuro Suzuki (Department of Virology II, National Institute of Infectious Diseases) for technical assistance with the 2D-DIGE. Grant support was received from Health and Labor Sciences Research Grants on HIV/AIDS and Measures for Intractable Diseases from the Ministry of Health, Labour, and Welfare (grants H15-AIDS-005 to HK and 17243601 to TS), a Grant-in-Aid for Scientific Research from the Ministry of Education, Culture, Sports, Science, and Technology of Japan (grant 17590365 to HK), a grant for Research on Health Sciences focusing on Drug Innovation from the Japan Health Sciences Foundation (grant SA14831 to HK), and a grant from the New Energy and Industrial Technology Development Organization (NEDO; grant to SW).

Supplementary material

Supplementary material may be found at the web address http://www.interscience.wiley.com/jpages/0022-3417/suppmat/path.2012.html.

References

1. Cesarman E, Chang Y, Moore PS, Said JW, Knowles DM. Kaposi's sarcoma-associated herpesvirus-like DNA sequences in AIDS-related body-cavity-based lymphomas. *N Engl J Med* 1995;**332**:1186–1191.
2. Nador RG, Cesarman E, Chadburn A, Dawson DB, Ansari MQ, Sald J, *et al*. Primary effusion lymphoma: a distinct clinicopathologic entity associated with the Kaposi's sarcoma-associated herpes virus. *Blood* 1996;**88**:645–656.
3. Knowles DM, Inghirami G, Ubriaco A, Dalla-Favera R. Molecular genetic analysis of three AIDS-associated neoplasms of uncertain lineage demonstrates their B-cell derivation and the possible pathogenetic role of the Epstein-Barr virus. *Blood* 1989;**73**:792–799.
4. Banks PM, Warnke RA. *Primary Effusion Lymphoma*. IARC Press: Lyon, 2001.
5. Katano H, Sato Y, Kurata T, Mori S, Sata T. Expression and localization of human herpesvirus 8-encoded proteins in primary effusion lymphoma, Kaposi's sarcoma, and multicentric Castleman's disease. *Virology* 2000;**269**:335–344.
6. Parravicini C, Chandran B, Corbellino M, Berti E, Paulli M, Moore PS, *et al*. Differential viral protein expression in Kaposi's sarcoma-associated herpesvirus-infected diseases: Kaposi's sarcoma, primary effusion lymphoma, and multicentric Castleman's disease. *Am J Pathol* 2000;**156**:743–749.

7. Dupin N, Fisher C, Kellam P, Ariad S, Tulliez M, Franck N, *et al*. Distribution of human herpesvirus-8 latently infected cells in Kaposi's sarcoma, multicentric Castleman's disease, and primary effusion lymphoma. *Proc Natl Acad Sci USA* 1999;**96**:4546–4551.
8. Chadburn A, Hyjek E, Mathew S, Cesarman E, Said J, Knowles DM. KSHV-positive solid lymphomas represent an extra-cavitary variant of primary effusion lymphoma. *Am J Surg Pathol* 2004;**28**:1401–1416.
9. Carbone A, Gloghini A, Vaccher E, Cerri M, Gaidano G, Dalla-Favera R, *et al*. Kaposi's sarcoma-associated herpesvirus/human herpesvirus type 8-positive solid lymphomas: a tissue-based variant of primary effusion lymphoma. *J Mol Diagn* 2005;**7**:17–27.
10. Katano H, Suda T, Morishita Y, Yamamoto K, Hoshino Y, Nakamura K, *et al*. Human herpesvirus 8-associated solid lymphomas that occur in AIDS patients take anaplastic large cell morphology. *Mod Pathol* 2000;**13**:77–85.
11. Boshoff C, Gao SJ, Healy LE, Matthews S, Thomas AJ, Coignet L, *et al*. Establishing a KSHV+ cell line (BCP-1) from peripheral blood and characterizing its growth in Nod/SCID mice. *Blood* 1998;**91**:1671–1679.
12. Rocha M, Kruger A, Umansky V, von Hoegen P, Naor D, Schirrmacher V. Dynamic expression changes in vivo of adhesion and costimulatory molecules determine load and pattern of lymphoma liver metastasis. *Clin Cancer Res* 1996;**2**:811–820.
13. Drillenburg P, Pals ST. Cell adhesion receptors in lymphoma dissemination. *Blood* 2000;**95**:1900–1910.
14. Roos E. Adhesion molecules in lymphoma metastasis. *Semin Cancer Biol* 1993;**4**:285–292.
15. Katagiri K, Maeda A, Shimonaka M, Kinashi T. RAPL, a Rap1-binding molecule that mediates Rap1-induced adhesion through spatial regulation of LFA-1. *Nat Immunol* 2003;**4**:741–748.
16. Giagulli C, Scarpini E, Ottoboni L, Narumiya S, Butcher EC, Constantin G, *et al*. RhoA and zeta PKC control distinct modalities of LFA-1 activation by chemokines: critical role of LFA-1 affinity triggering in lymphocyte in vivo homing. *Immunity* 2004;**20**:25–35.
17. Rodriguez-Fernandez JL, Gomez M, Luque A, Hogg N, Sanchez-Madrid F, Cabanas C. The interaction of activated integrin lymphocyte function-associated antigen 1 with ligand intercellular adhesion molecule 1 induces activation and redistribution of focal adhesion kinase and proline-rich tyrosine kinase 2 in T lymphocytes. *Mol Biol Cell* 1999;**10**:1891–1907.
18. Vyth-Dreese FA, Dellemijn TA, van Oostveen JW, Feltkamp CA, Hekman A. Functional expression of adhesion receptors and costimulatory molecules by fresh and immortalized B-cell non-Hodgkin's lymphoma cells. *Blood* 1995;**85**:2802–2812.
19. Hamilton-Dutoit SJ, Rea D, Raphael M, Sandvej K, Delecluse HJ, Gisselbrecht C, *et al*. Epstein-Barr virus-latent gene expression and tumor cell phenotype in acquired immunodeficiency syndrome-related non-Hodgkin's lymphoma. Correlation of lymphoma phenotype with three distinct patterns of viral latency. *Am J Pathol* 1993;**143**:1072–1085.
20. Peng M, Lundgren E. Transient expression of the Epstein-Barr virus LMP1 gene in human primary B cells induces cellular activation and DNA synthesis. *Oncogene* 1992;**7**:1775–1782.
21. Wang D, Liebowitz D, Wang F, Gregory C, Rickinson A, Larson R, *et al*. Epstein-Barr virus latent infection membrane protein alters the human B-lymphocyte phenotype: deletion of the amino terminus abolishes activity. *J Virol* 1988;**62**:4173–4184.
22. Fukudome K, Furuse M, Fukuhara N, Orita S, Imai T, Takagi S, *et al*. Strong induction of ICAM-1 in human T cells transformed by human T-cell-leukemia virus type 1 and depression of ICAM-1 or LFA-1 in adult T-cell-leukemia-derived cell lines. *Int J Cancer* 1992;**52**:418–427.
23. Tanaka Y, Fukudome K, Hayashi M, Takagi S, Yoshie O. Induction of ICAM-1 and LFA-3 by Tax1 of human T-cell leukemia virus type 1 and mechanism of down-regulation of ICAM-1 or LFA-1 in adult-T-cell-leukemia cell lines. *Int J Cancer* 1995;**60**:554–561.
24. Drexler HG, Uphoff CC, Gaidano G, Carbone A. Lymphoma cell lines: in vitro models for the study of HHV-8+ primary effusion lymphomas (body cavity-based lymphomas). *Leukemia* 1998;**12**:1507–1517.
25. Suscovich TJ, Paulose-Murphy M, Harlow JD, Chen Y, Thomas SY, Mellott TJ, *et al*. Defective immune function of primary effusion lymphoma cells is associated with distinct KSHV gene expression profiles. *Leuk Lymphoma* 2004;**45**:1223–1238.
26. Katano H, Pesnicak L, Cohen JI. Simvastatin induces apoptosis of Epstein-Barr virus (EBV)-transformed lymphoblastoid cell lines and delays development of EBV lymphomas. *Proc Natl Acad Sci USA* 2004;**101**:4960–4965.
27. Katano H, Hoshino Y, Morishita Y, Nakamura T, Satoh H, Iwamoto A, *et al*. Establishing and characterizing a CD30-positive cell line harboring HHV-8 from a primary effusion lymphoma. *J Med Virol* 1999;**58**:394–401.
28. Alban A, David SO, Bjorkesten L, Andersson C, Sloge E, Lewis S, *et al*. A novel experimental design for comparative two-dimensional gel analysis: two-dimensional difference gel electrophoresis incorporating a pooled internal standard. *Proteomics* 2003;**3**:36–44.
29. Evans CA, Tonge R, Blinco D, Pierce A, Shaw J, Lu Y, *et al*. Comparative proteomics of primitive hematopoietic cell populations reveals differences in expression of proteins regulating motility. *Blood* 2004;**103**:3751–3759.
30. Shevchenko A, Wilm M, Vorm O, Mann M. Mass spectrometric sequencing of proteins silver-stained polyacrylamide gels. *Anal Chem* 1996;**68**:850–858.
31. Ito E, Honma R, Imai J, Azuma S, Kanno T, Mori S, *et al*. A tetraspanin-family protein, T-cell acute lymphoblastic leukemia-associated antigen 1, is induced by the Ewing's sarcoma-Wilms' tumor 1 fusion protein of desmoplastic small round-cell tumor. *Am J Pathol* 2003;**163**:2165–2172.
32. Kobayashi S, Ito E, Honma R, Nojima Y, Shibuya M, Watanabe S, *et al*. Dynamic regulation of gene expression by the Flt-1 kinase and Matrigel in endothelial tubulogenesis. *Genomics* 2004;**84**:185–192.
33. Fakhari FD, Dittmer DP. Charting latency transcripts in Kaposi's sarcoma-associated herpesvirus by whole-genome real-time quantitative PCR. *J Virol* 2002;**76**:6213–6223.
34. White IE, Campbell TB. Quantitation of cell-free and cell-associated Kaposi's sarcoma-associated herpesvirus DNA by real-time PCR. *J Clin Microbiol* 2000;**38**:1992–1995.
35. Lallemand F, Desire N, Rozenbaum W, Nicolas JC, Marechal V. Quantitative analysis of human herpesvirus 8 viral load using a real-time PCR assay. *J Clin Microbiol* 2000;**38**:1404–1408.
36. Katano H, Sato Y, Itoh H, Sata T. Expression of human herpesvirus 8 (HHV-8)-encoded immediate early protein, open reading frame 50, in HHV-8-associated diseases. *J Hum Virol* 2001;**4**:96–102.
37. Griffiths EK, Penninger JM. Communication between the TCR and integrins: role of the molecular adapter ADAP/Fyb/Slap. *Curr Opin Immunol* 2002;**14**:317–322.
38. Kinashi T, Katagiri K. Regulation of lymphocyte adhesion and migration by the small GTPase Rap1 and its effector molecule, RAPL. *Immunol Lett* 2004;**93**:1–5.
39. Jenner RG, Maillard K, Cattini N, Weiss RA, Boshoff C, Wooster R, *et al*. Kaposi's sarcoma-associated herpesvirus-infected primary effusion lymphoma has a plasma cell gene expression profile. *Proc Natl Acad Sci USA* 2003;**100**:10 399–10 404.
40. Aoki Y, Jaffe ES, Chang Y, Jones K, Teruya-Feldstein J, Moore PS, *et al*. Angiogenesis and hematopoiesis induced by Kaposi's sarcoma-associated herpesvirus-encoded interleukin-6. *Blood* 1999;**93**:4034–4043.
41. Aoki Y, Narazaki M, Kishimoto T, Tosato G. Receptor engagement by viral interleukin-6 encoded by Kaposi sarcoma-associated herpesvirus. *Blood* 2001;**98**:3042–3049.
42. Aoki Y, Tosato G. Targeted inhibition of angiogenic factors in AIDS-related disorders. *Curr Drug Targets Infect Disord* 2003;**3**:115–128.
43. Suzuki K, Nishihata J, Arai Y, Honma N, Yamamoto K, Irimura T, *et al*. Molecular cloning of a novel actin-binding protein, p57, with a WD repeat and a leucine zipper motif. *FEBS Lett* 1995;**364**:283–288.

J Pathol 2006; **209**: 464–473 DOI: 10.1002/path

44. Rybakin V, Clemen CS. Coronin proteins as multifunctional regulators of the cytoskeleton and membrane trafficking. *Bioessays* 2005;**27**:625–632.
45. Nal B, Carroll P, Mohr E, Verthuy C, Da Silva MI, Gayet O, *et al*. Coronin-1 expression in T lymphocytes: insights into protein function during T cell development and activation. *Int Immunol* 2004;**16**:231–240.
46. Roesch Ely M, Nees M, Karsai S, Magele I, Bogumil R, Vorderwulbecke S, *et al*. Transcript and proteome analysis reveals reduced expression of calgranulins in head and neck squamous cell carcinoma. *Eur J Cell Biol* 2005;**84**:431–444.
47. Yim EK, Meoyng J, Namakoong SE, Um SJ, Park JS. Genomic and proteomic expression patterns in HPV-16 E6 gene transfected stable human carcinoma cell lines. *DNA Cell Biol* 2004;**23**:826–835.
48. Hall N, Karras M, Raine JD, Carlton JM, Kooij TW, Berriman M, *et al*. A comprehensive survey of the Plasmodium life cycle by genomic, transcriptomic, and proteomic analyses. *Science* 2005;**307**:82–86.

研究成果の刊行に関する一覧表

雑誌

発表者氏名	論文タイトル名	発表誌名	巻号	ページ	出版年
KHALIFA S.A.M., IMAI E., KOBAYASHI S., HAGHIGHI A., HAYAKAWA E. & TAKEUCHI T.	GROWTH-PROMOTING EFFECT ON IRON-SULFUR PROTEINS ON AXENIC CULTURES OF ENTAMOEBA DISPAR	Parasite	13	51-58	2006
鈴木　淳 村田理恵 柳川義勢 小林正規 竹内　勤	知的障害者更生施設における赤痢アメーバ等腸管寄生原虫の感染実態調査(2) －E.disparの施設内感染を中心として－	Clinical Parasitology	17	52-55	2006
Masaharu Tokoro, Kentaro Nakamoto, Amjad I. A. Hussein, Tomoko Arai	Genotyping of Cryptosporidium species: current status and future direction	Parasitic Zoonoses in Asian-Pacific Regions		3-7	2006
所　正治 吉田知代 荒井朋子 井関基弘 古川　博 小松八千代	PCR法によるサイクロスポーラの検出と種の同定	Clinical Parasitology	17	145-148	2006
所　正治 井関基弘	クリプトスポリジウム症	G.I.Research	14	20-25	2006

書籍

著者氏名	論文タイトル	書籍全体の編集者	書籍名	出版社名	出版地	ページ	出版年
T. Asai and S. Tomavo	Biochemistry and Metabolism of Toxoplasma gondii	Weiss & Kim	Toxoplasma gondii. The Model Apicomplexan-Perspectives and Methods	Elsevier Science	London	185-206	2006

GROWTH-PROMOTING EFFECT ON IRON-SULFUR PROTEINS ON AXENIC CULTURES OF *ENTAMOEBA DISPAR*

KHALIFA S.A.M.*, IMAI E.*, KOBAYASHI S.*, HAGHIGHI A.**, HAYAKAWA E.* & TAKEUCHI T.*

Summary:

A growth-promoting factor (GPF) that promotes the growth of *Entamoeba dispar* under axenic culture conditions was found in fractions of mitochondria (Mt), hydrogenosomes (Hg) and chloroplasts (Cp) obtained from cells of six different protozoan, mammalian and plant species. We were able to extract the GPF from the Cp-rich leaf cells of a plant (spiderwort: *Commelina communis* L.) in an acetone-soluble fraction as a complex of chlorophyll with low molecular weight proteins (molecular weight [MW] approximately 4,600). We also found that on treatment with 0.6 % complexes of 2-mercapthoethanol (2ME), complexes of chlorophyll-a with iron-sulphur (Fe-S) proteins (e.g., ferredoxins [Fd] from spinach and *Clostridium pasteurianum*) and noncomplex rubredoxin (Rd) from *C. pasteurianum* have a growth-promoting effect on *E. dispar*. These findings suggest that *E. dispar* may lack a sufficient quantity of some essential components of Fe-S proteins, such as Fe-S center.

KEY WORDS : growth, mitochondria, hydrogenosomes, chloroplasts, iron-sulphur protein, *Entamoeba dispar*.

Résumé : LES EFFETS D'ACCÉLÉRATION DE CROISSANCE DES PROTÉINES FER-SOUFRE DANS LA CULTURE AXÉNIQUE D'*ENTAMOEBA DISPAR*

Des facteurs d'accélération de croissance (Growth promoting factor: GPF) favorisant le développement d'Entamoeba dispar ont été détectés dans la composition de la mitochondrie, de l'hydrogénosome et du chloroplaste isolés à partir de six sortes de cellules issues de protozoaires, mammifères et plantes. De plus, les GPF de cellules de mésophile contenant une grande quantité de chloroplaste végétal (Commelina communis L.) ont pu être extraits comme une substance composée de protéines de faible masse moléculaire (= 4600) et de chloroplastes dans la composition acétone-soluble. À partir de ces résultats, nous avons préalablement pu découvrir des effets d'accélération de croissance dans le corps composé de protéines fer-soufre (épinard et ferrédoxine de Clostridium pasteurianum) et de chlorophylle-a traité au 2-mercaptoéthanol 0,6 % et du corps simple rubrédoxine de C. pasteurianum. Ces observations ont suggéré qu'une composante essentielle formant la protéine fer-soufre d'E. dispar (comme noyau fer-soufre) semblait être insuffisante.

MOTS CLÉS : *croissance, mitochondrie, hydrogénosome, chloroplaste, protéine fer-soufre, Entamoeba dispar.*

INTRODUCTION

Entamoeba dispar grows well under xenic and monoxenic culture conditions along with enteric bacteria such as *Escherichia coli* or anaerobic bacteria such as *Fusobacterium symbiosum* (*Clostridium symbiosum* ATCC 14940) (Robinson, 1968; Diamond, 1982; Vargas *et al.*, 1990). However, even after the introduction of the axenic yeast extract-iron serum (YI-S) medium for *E. dispar* (Diamond *et al.*, 1995; Clark, 1995) the axenic cultivation of *E. dispar* remains difficult. Compared with *E. dispar*, pathogenic *E. histolytica*, which is closely related to *E. dispar*, easily adapts to the axenic culture medium (TYI-S-33) (Diamond *et al.*, 1978). Additionally, *Entamoeba histolytica* is capable of invading the mucosa of the large intestine. We have also developed a new yeast extract-iron-gluconic acid-dihydroxyacetone-serum medium (YIGADHA-S) (Kobayashi *et al.*, 2005) based on the YI-S medium and on the results of an investigation on bacterial metabolic products, and have succeeded in culturing five strains under axenic conditions. However, despite using the YIGADHA-S culture system, the axenic growth of four of five strains of *E. dispar* was found to be very poor, with the exception of one primate-derived strain (CYNO 09: TPC) isolated from a cynomolgus monkey. A further search for useful growth promoting factors (GPFs) revealed that autoclaved (121° C, 15 minutes) bacteria and more than 20 types of protozoan, mammalian and plant cells containing mitochondria (Mt), hydrogenosomes (Hg) and chloroplasts (Cp) have a significant growth-promoting effect on *E. dispar*. However, the degree of these growth-promoting effects differs among the GPFs. In the present study, we were able to extract GPF from the Cp-rich leaf cells of a plant (spiderwort: *Commelina communis* L.) in an acetone-soluble fraction as a chlorophyll complex with low mole-

* Department of Tropical Medicine and Parasitology, School of Medicine, Keio University, Shinjuku-ku, Tokyo, Japan.
** Department of Medical Parasitology and Mycology, School of Medicine Shaheed University of Medical Sciences, Eveen, Teheran 19395, Iran.
Correspondence: Seiki Kobayashi, PhD., Department of Tropical Medicine and Parasitology, School of Medicine, Keio University, 35 Shinanomachi, Shinjuku-ku, Tokyo 160-8582, Japan.
Tel.: +81-3-5363-3761 – Fax: +81-3-3353-5958.
E-mail: skobaya@sc.itc.keio.ac.jp

cular weight proteins. Significant amounts of iron (Fe), sulphur (S) and molybdenum (Mo) atoms were found in the protein-chlorophyll complex fraction along with the magnesium (Mg) atom of chlorophyll.

Based on these findings, we hypothesized that some common components of Fe-S proteins present in Mt, Hg, Cp and bacteria support the growth of *E. dispar*. This is because in *E. dispar*, an essential redox Fe-S protein [ferredoxin (Fd)] is expected to be involved in energy metabolism, such as oxidative decarboxylation of pyruvate to acetyl-coenzyme A (acetyl-CoA), which is similar to that found in *E. histolytica* (McLaughlin & Aley, 1985).

MATERIALS AND METHODS

E. DISPAR ISOLATE

In this study, one human-derived strain of axenically grown *E. dispar* (AS 16 IR) (Kobayashi *et al.*, 2005) was used to determine the growth promoting effect of Fe-S proteins.

AXENIC CULTIVATION OF *E. DISPAR*

The YIGADHA-S medium (Kobayashi *et al.*, 2005) containing 15 % heat-inactivated bovine serum was used as the axenic cultivation medium for *E. dispar*.

DONOR CELLS OF MT, HG, CP AND MITOSOMES

The Mt donors are as follows: protozoan parasites: i) *Crithidia fasciculata* (ReF-1, PRR strain, ATCC 50083); ii) *Trypanosoma cruzi* (Tulahuen strain); iii) *Leishmania major* (MHOM/SU/73/5-ASKH strain, ATCC 50155); and iv) *Acanthamoeba castellanii* (ATCC 30011). v) The vertebrate cells used as Mt donors were from the mouse lymphoblast cell line (P388D1, ATCC CCL-46). The Hg donors are as follows: protozoan parasites: vi) *Trichomonas vaginalis* (KO-11 strain) (Qi *et al.*, 1995) and vii) *Trichomonas foetus* (Okamoto *et al.*, 1998). viii) Leaves of the spiderwort (*Commelina communis* L.) were used as the Cp donors. Consisting amitochondrial protozoan parasite mitosomes that are mitochondrial remnant organelles (Tovar *et al.*, 2003) was used as the mitosome donor, ix) *Giardia intestinalis* (syn. *lamblia*), (Portland-I strain, ATCC 30888). The bacterium used was *Pseudomonas aeruginosa* (PA:KEIO strain) (Kobayashi *et al.*, 1998).

PREPARATION OF CELLS

C. fasciculata and *T. cruzi* were axenically cultured in liver infusion tryptose (LIT) medium (*Gutteridge et al.*, 1969) supplemented with 10 % foetal bovine serum (FBS). After cultivation for three and seven days respectively, 2×10^7 cells of each parasite were harvested by centrifugation (650 g × 8 minutes). The cells of each parasite were washed three times by centrifugation with 10 mM phosphate-buffered saline (PBS) (pH 7.4), and each pellet was suspended in approximately eight times its volume of 50 mM Tris-HCl (pH 7.4). *L. major* was axenically cultured in Schneider's medium (Gibco™) supplemented with 15 % FBS at 26° C for four days and harvested by centrifugation (650 g × 8 minutes). *A. castellanii* was axenically cultured in peptone-yeast glucose (PYG) medium (Rowbotham, 1983; ATCC media formulations No. 712) for four days and harvested by centrifugation (650 g × 4 minutes). The P388D1 cell line was cultured in RPMI 1640 medium (Nissui Pharmaceutical Co., Taito-ku, Tokyo, Japan) supplemented with 10 % FBS for four days and harvested by centrifugation (125 g × 4 minutes). *T. vaginalis* and *T. foetus* were axenically cultured for three days in BI-S-33 medium in which the peptone components of TYI-S-33 medium (Diamond *et al.*, 1978) are substituted by Biosate (BBL, Becton Dickinson Co., Cockeysville, Maryland, USA), and harvested by centrifugation (275 g × 4 minutes). The Cp-rich fraction from the wild spiderwort (*C. communis* L.) was isolated. The leaves of wild spiderwort were picked from the private field of Keio University (Tokyo) during the flower season from June to August (2000-2003). Fresh green spiderwort leaves were stripped from the stems, washed with tap water and then with distilled water. The leaves were ground with serum-free RPMI 1640 medium (RPMI) in an earthenware mortar by using a wooden pestle. The resulting leaf cell suspension was filtered through a double thickness gauze to remove the residue. The cell suspension was then washed three times with RPMI by centrifugation (440 g × 10 minutes). *P. aeruginosa* was cultured in Biosate-Iron broth (Diamond *et al.*, 1978) for three days and harvested by centrifugation (650 g × 4 minutes). *G. intestinalis* was axenically cultured in modified BI-S-33 medium (Keister, 1983) for three days and harvested by centrifugation (275 g × 4 minutes).

PREPARATION OF MT, HG AND CP FRACTIONS

Mt, Hg and Cp rich fractions were prepared as described by Hogeboom (1955), Opperdoes *et al.* (1984) and Gorham (1955), respectively. Since the methodology for mitosome isolation has not been established, intact cells of *G. intestinalis* were tested for their growth-promoting effect without preparing the mitosome rich fraction. After washing the fractions with RPMI once by centrifugation (440 g × 10 minutes), each fraction was suspended in 2 ml of RPMI. In order to test for their growth-promoting effect under axenic culture conditions, the fractions were sterilized by autoclaving (121° C, 15 minutes), and 0.2 ml of each suspension was added into the YIGADHA-S medium (5 ml). The

medium was then inoculated with a 0.8 ml suspension of *E. dispar* (AS16IR strain = AS 16 IR) (final density: 200-2,700 amoebae/ml).

NuPAGE® Novex 4-12 % Bis-Tris gradient peptide gel electrophoresis and preparative sodium dodecyl sulfate-polyacrylamide gel electrophoresis (SDS-PAGE)

The lyophilized cell fraction of spiderwort was extracted with 20 %, 40 %, 80 % and 100 % acetone solutions (20 mg/ml) for 10 minutes at 4° C. After centrifugation (17,800 g × 10 minutes, 4° C) of each acetone extract, the supernatant was collected. The supernatants that were extracted with 80 % and 100 % acetone solutions were diluted with distilled water to obtain an acetone concentration of 50 %. Each supernatant was then concentrated by evaporation by using a SpeedVac system (SVC 100; Savant Instruments, Inc., Farmingdale, New York, USA) until evaporated to dryness. The molecular weight of the proteins in each extract was determined by NuPAGE® Novex 4-12 % Bis-Tris gradient peptide (Invitrogen Corp., Carlsbad, California, USA) gel electrophoresis.

The bands of complexes of low molecular weight protein with chlorophyll that were detected in the supernatants of 80 % and 100 % acetone extracts were isolated by preparative SDS-PAGE on a 12 % gel in a Mini Prep Cell (Bio-Rad Laboratories, Inc., Hercules, California, USA) electrophoresis unit. SDS-PAGE was performed according to the procedure described by Laemmli (1970). For NuPAGE® (Novex 4-12 % gradient peptide gel = Novex 4-12 %) each dried and concentrated supernatant of the acetone extract was redissolved in the sample buffer with 50 mM dithiothreitol and heated at 70° C for 10 minutes to reduce the disulfide bonds. For SDS-PAGE (12 % gel) each supernatant was redissolved in the sample buffer with 1 % (v/v) 2-mercaptoethanol (2ME) and boiled for four minutes. Following NuPAGE®, the gel was stained with 2D-silverstain II (Daiichi Pure Chemicals Co. Ltd., Chuo-ku, Tokyo, Japan).

Assay of the acetone extracts of spiderwort leaf cells for a GPF

One millilitre supernatants (obtained after centrifugation; 17,800 g × 10 minutes, 4° C) of the 20 %, 40 %, 80 % and 100 % acetone extracts of the lyophilized cell fraction of spiderwort (20 mg/ml) was dialyzed three times against 200-250 volumes of distilled water for 18 hours by using a Spectra/Por® 3 (3500 MWCO) dialysis membrane for 18 h; the volume of each extract was adjusted to 2.4 ml. Each extract was sterilized by filtration (Sartorius membrane filter; 0.2-µm pore size), and 0.2 ml of each extract was added to the YIGADHA-S medium to test the growth-promoting effect of the extract on *E. dispar* (AS 16 IR).

Analysis using a scanning electron microscopy (SEM)/energy dispersive X-ray analyser (EDX)-integrated analysis system

Following the preparative SDS-PAGE, the complexes of chlorophyll with low molecular weight proteins in the 80 % and 100 % acetone-soluble fractions were dialyzed in the same manner as described above. After lyophilization, the dialyzed complexes were examined using an SEM and EDX-integrated analysis system SEM-EDX III Type N/H (Hitachi Science Systems, Ltd., Hitachinaka, Ibaragi, Japan) in the Nihonbashi laboratory, Hitachi High-Technologies Co., Tokyo, Japan.

Preparation of chlorophyll-a complexes with purified iron-sulphur proteins

Purified Fd from spinach (1 µg/µl; Sigma F-3013) and *C. pasteurianum* (1 µg/µl; Sigma F-7629) and purified rubredoxin (Rd) from *C. pasteurianum* (15.7 µg/µl; Sigma R-2512) were dissolved in 0.6 % 2ME/H_2O (20 µg of Fd or 31.4 µg of Rd/4 ml of 0.6 % 2ME), and the Fd and Rd solutions were dialyzed in the same manner as described above. Purified chlorophyll-a (Sigma C-5753) was dissolved in acetone (25 µg/25 µl acetone), and after adding 4 ml of distilled water, the solution was dialyzed in the same manner as described above. The Fd and Rd solutions were mixed with dialyzed chlorophyll-a and incubated for 10 minutes at 25° C. The solutions of chlorophyll-a complexes were then sterilized by filtration, and 0.2 ml of each solution was added to the YIGADHA-S medium to test their growth-promoting effect on *E. dispar* AS 16 IR.

Statistical analysis of growth-promoting effect on *E. dispar*

All experiments for testing growth-promoting effect were repeated at least twice. The data of each experiment were subjected to one-way analysis of variance (ANOVA) with Dunnett's multiple comparison post hoc test; the levels of statistical significance were taken as $p < 0.05$ and $p < 0.01$.

RESULTS

The Mt, Hg and Cp isolated from eight different types of cells were tested to determine whether they promoted the growth of axenically grown *E. dispar* AS 16 IR. The intact cells of *G. intestinalis* and *P. aeruginosa* were also tested for the same. A growth-promoting effect was apparently observed for every fraction except for the fraction of intact cells of *G. intestinalis*. Apparently, the intact cells of *E. histolytica* (HM-1: IMSS clone 6 strain) containing mitosomes (Leon-Avila & Tovar, 2004) also did not produce a

growth-promoting effect (data not shown). Although the growth-promoting effect of the two fractions of Mt from *T. cruzi* and the Hg fraction from *T. vaginalis* retained the statistically significant difference by Dunnett's test ($p < 0.05$), the growth-promoting effect of the other six fractions containing Mt, Hg and Cp was significantly different ($p < 0.01$ or $p < 0.05$). In particular, the effect of the Cp fraction from spiderwort exceeded that of the intact cells fraction of *P. aeruginosa* as shown in Figure 1. Thus, it was concluded that some of the Mt, Hg and Cp fractions, which were obtained under appropriate conditions as well as the intact bacterial cells contain a GPF.

Acetone extraction was used to obtain a water-soluble GPF from Cp-rich leaf cells of some plant species (e.g., spiderwort, cherry and morning glory), which have sufficiently strong leaf-cell membranes that can withstand the leaf crushing and cell isolation process. Figure 2 shows the results obtained on testing the 0 %, 20 %, 40 %, 80 % and 100 % acetone-soluble fractions from lyophilized Cp-rich leaf cells of spiderwort for a growth-promoting effect. The results showed that the 20 % and 80 % acetone-soluble fractions had a stronger growth-promoting effect than the other acetone-soluble fractions (0 %, 40 % and 100 %). The growth-promoting effects of the 20 % and 80 % acetone-soluble fractions were statistically significant at $p < 0.01$ (Dunnett's test); however, the effects of the 0 %, 40 % and 100 % acetone-soluble fractions were retained at $p < 0.05$. The silverstain NuPAGE® analysis of these acetone-soluble fractions yielded a distinct dense protein band (MW 4600) that was common to the 20 %, 40 %, 80 % and 100 % acetone-soluble fractions. The intensity of the bands of the 20 % and 80 % acetone-soluble fractions were stronger than the bands of the other acetone-soluble fractions (40 % and 100 %) (Fig. 3). These results indicated that the efficacy of the growth-promoting effect was correlated with the intensity of the low molecular weight protein band (Figs 2, 3). The band of the complex of the chlorophyll with low molecular weight proteins (green colour) present in both the 80 % and 100 % acetone-soluble fractions was obtained by SDS-preparative electrophoresis; both the fractions showed a growth-promoting effect on *E. dispar* AS 16 IR (data not shown). The result showed that the band of the complex of chlorophyll with low molecular weight proteins, which was present in the acetone-soluble fractions, contained a GPF. The reduction in the intensity of the low molecular weight protein bands obtained by using the 40 % acetone-soluble fraction was considered to be caused by the incomplete solubility of chlorophyll. Some protein parts are believed to be precipitated together with the insoluble chlorophyll when extraction is performed with an intermediate concen-

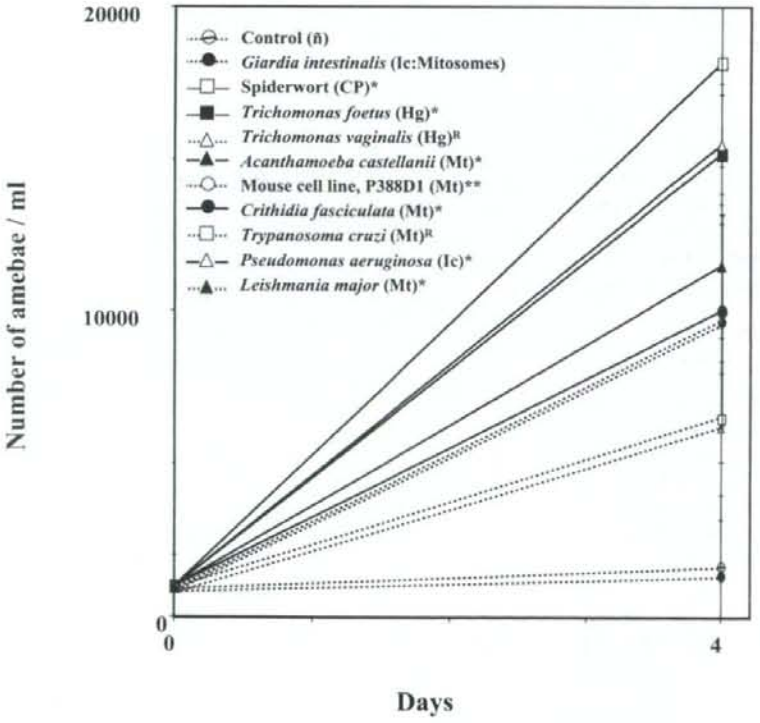

Fig. 1. – The effect of intact cells (Ic) and the fractions of mitochondria (Mt), chloroplasts (Cp) and hydrogenosomes (Hg) from ten types of cells, including bacterial, mammalian, plant and protozoan cells, on the growth of *Entamoeba dispar*.

The cellular components were sterilized by autoclaving at 121° C for 15 minutes. The growth kinetics of the *E. dispar* AS 16 IR strain in the YIGADHA-S medium are shown (mean numbers of amoebae in duplicate cultures are plotted). *, **: the mean of the growth-kinetic level was significantly higher than that of the control (*$p < 0.01$ and **$p < 0.05$ by Dunnett's test). R: the significant difference was retained by Dunnett's test ($p < 0.05$).

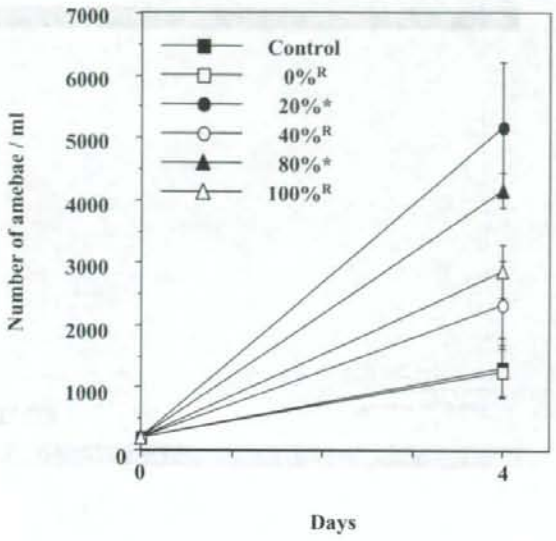

Fig. 2. – Effect of soluble fractions of spiderwort Cp-rich leaf cells extracted with five different concentrations of acetone (0 %, 20 %, 40 %, 80 % and 100 %) on the growth of *E. dispar*.
The growth kinetics of the *E. dispar* AS 16 IR strain in the YIGADHA-S medium are shown (mean numbers of amoebae in duplicate cultures are plotted). *: the mean of the growth-kinetic level was significantly higher than that of the control (*$p < 0.01$ by Dunnett's test). R: the significant difference was retained by Dunnett's test ($p < 0.05$).

tration of acetone such as 40 %. As compared to an 80 % acetone concentration, the 100 % concentration of acetone was considered to be slightly severe for the extraction of the low molecular weight proteins without decreasing the activity of a GPF. As a result, the intensity of the low molecular weight protein bands obtained by using the 40 % and 100 % acetone-soluble fraction was believed to be reduced.

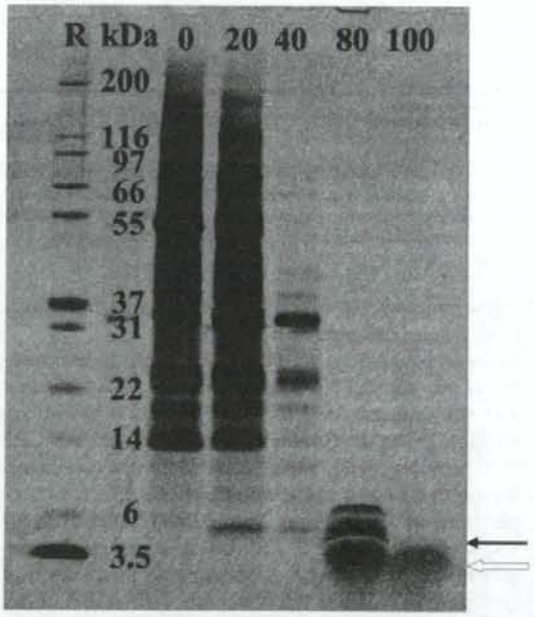

Fig. 3. – NuPAGE® (Novex 4-12 %) of five acetone-soluble fractions of spiderwort Cp-rich leaf cells extracted with different concentrations of acetone (0 %, 20 %, 40 %, 80 % and 100 %).
Molecular mass markers (M) are shown on the left. ⟵ : acetone-soluble low molecular weight protein bands were isolated from the 20 %, 40 %, 80 % and 100 % acetone-soluble fractions. ⇦: broad green band of chlorophyll.

The SEM/EDX-integrated analysis system revealed that the low molecular weight protein band contained Fe, S and Mo atoms along with the Mg atom of chlorophyll (Figs 4, 5). We believed that Fd present in Cp is a type of Fe-S protein containing Fe and S atoms. In order to confirm the growth-promoting effect of Fd, we examined the effects of purified spinach Fd (MW 12,000), *C. pasteurianum* Fd (MW 6,000) and purified *C. pasteurianum* Rd (MW 19,000) on the growth of *E. dispar* AS 16 IR. The analysis revealed that 0.6 % 2ME-treated *C. pasteurianum* Rd and each of the water-soluble chlorophyll-a complexes with 0.6 % 2ME-treated spinach Fd and *C. pasteurianum* Fd have a growth-promoting effect on *E. dispar* AS 16 IR with a statistically significant difference ($p < 0.01$) (Fig. 6). The non-complexed Fd from spinach and from *C. pasteurianum* treated with 0.6 % 2ME also had a slight growth-promoting effect when compared with the growth kinetics of the control with or without chlorophyll-a; however, these growth-promoting effects were retained ($p < 0.05$).

These results suggest that the GPF in the acetone-soluble fraction of spiderwort Cp-rich leaf cells is the complex of the chlorophyll-a with a component of an Fe-S protein, such as an inorganic Fe-S centre, released by the breakage of disulfide bonds due to treatment with 2ME. The Fe-S redox proteins are commonly found in enteric bacteria (e.g., Fd), mitochondria (e.g., Fe-S proteins in complex I and II), chloroplasts (e.g., Fd) and hydrogenosomes (e.g., Fd); however, there are diffe-

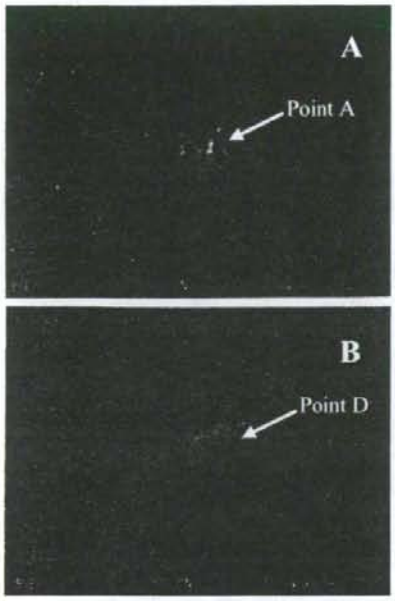

Fig. 4. – Scanning electron microscope (SEM) images of crystals observed in complexes of chlorophyll with low molecular weight proteins present in the 80 % (A) and 100 % (B) acetone-soluble fractions.
By using an SEM/energy dispersive X-ray (EDX) analyzer, Fe atoms were detected at point A (A) and S and Mo atoms were detected at point D (B).

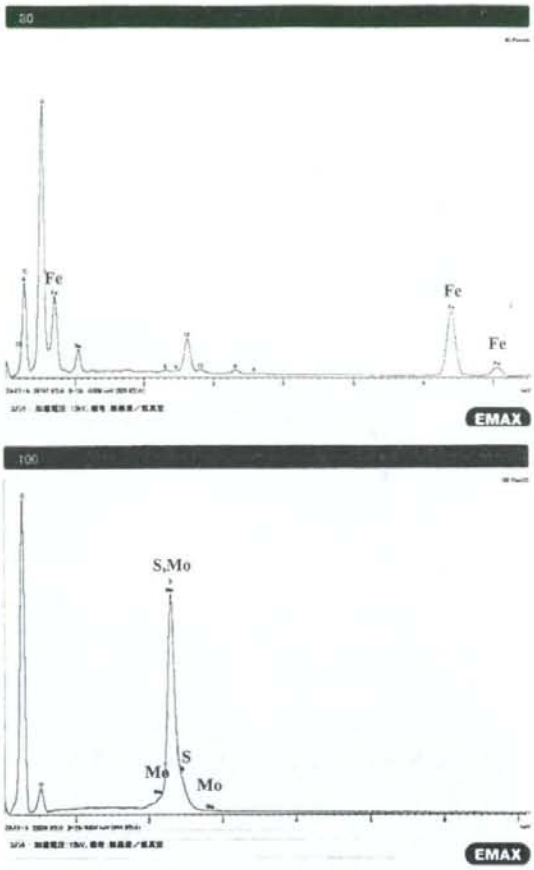

Fig. 5. – Specific peaks of the Fe atom at point A (Fig. 3) and S and Mo atoms at point D (Fig. 3) detected in the complexes of chlorophyll with low molecular weight proteins in the 80 % (A) and 100 % (B) acetone-soluble fractions by using an SEM/EDX analyzer.

rences in the chemical structure of their Fe-S centers. In *E. dispar*, Fd is considered as an essential redox protein involved in energy metabolism, similar to that in *E. histolytica*, although neither species contains Mt. These findings suggest that *E. dispar* grown under axenic culture conditions may lack a sufficient quantity of some essential component of the Fe-S proteins (e.g., Fe-S centre).
The growth-promoting effect of the GPF was tested on three other strains of *E. dispar* (SAW 1734R clone AR, AS 2 IR and CYNO 16:TPC), (Koyabashi *et al.*, 2005); it was confirmed that the GPF produced the same effect on their growth (data not shown).

DISCUSSION

Previously, we designed the YIGADHA-S medium (Kobayashi *et al.*, 2005) for axenic cultivation of *E. dispar*. It contains dihydroxyacetone (DHA) that has a significant growth-promoting effect on *E. dispar*. DHA is a ketotriose and functions as a sugar source for *E. dispar*, therefore, it is considered to be directly metabolized to DHA phosphate, which is an intermediary metabolite in the Embden-Meyerhof-Parnas glycolytic pathway. However, the growth of *E. dispar* was poor despite the presence of DHA.
In the present study, a GPF was detected in the autoclaved Mt, Hg and Cp fractions and in intact bacteria and was demonstrated to show a growth-promoting effect on *E. dispar*. However, the efficacy of each GPF from these organelles varied under different conditions. Prior to the present study, detection of a GPF from trophozoites of *E. histolytica* (HM-1:IMSS clone 6 strain) was attempted. Since *E. histolytica* is genetically closely related to *E. dispar*, it contains an abundance of Fe-S proteins, such as Fd, which are only stable under anaerobic conditions, and it contains mitochondrial remnant mitosomes (Leon-Avila & Tovar, 2004). However, neither the intact cells nor any extract from the cells could promote the growth of *E. dispar* AS 16 IR (data not shown). One reason for the failure to extract a GPF from *E. histolytica* trophozoites may be the fragility of